

## **Picodiscs for Facile Protein-Glycolipid Interaction Analysis**

Aneika C. Leney<sup>1,2</sup> Reza Rezaei Darestani,<sup>1,2</sup> Jun Li,<sup>1,2</sup> Sanaz Nikjah,<sup>1,2</sup> Elena N. Kitova,<sup>1,2</sup>  
Chunxia Zou,<sup>1,2</sup> Christopher W. Cairo,<sup>1,2</sup> Zi Jian Xiong,<sup>3</sup> Gilbert G. Privé,<sup>3,4</sup> John S. Klassen<sup>1,2\*</sup>

<sup>1</sup>*Alberta Glycomics Centre*

<sup>2</sup>*Department of Chemistry, University of Alberta, Edmonton, Alberta, Canada T6G 2G2*

<sup>3</sup>*Department of Biochemistry, University of Toronto, Toronto, Ontario, Canada M5S 1A8*

<sup>4</sup>*Princess Margaret Cancer Centre, University Health Network, Toronto, Ontario, Canada*

*M5G 1L7*

## **Abstract**

Protein interactions with glycolipids are implicated in diverse cellular processes. However, the study of protein-glycolipid complexes remains a significant experimental challenge. Here, we describe a powerful new assay that combines electrospray ionization mass spectrometry (ESI-MS) and picodiscs, which are composed of human sphingolipid activator protein saposin A and a small number of phospholipids, to display glycolipids in a lipid environment for protein-glycolipid interaction studies in aqueous solution. Time-resolved measurements of enzyme catalyzed hydrolysis of glycolipid substrates and the detection of low, moderate and high affinity protein–glycolipid interactions serve to demonstrate the reliability and versatility of the assay.

## Introduction

Many vital cellular processes, such as pathogen recognition, signalling, development and differentiation, rely on non-covalent interactions between proteins and glycolipid receptors.<sup>1-5</sup> Despite their biological importance, protein-glycolipid interactions are considerably under investigated and it is likely that many biologically-relevant interactions have yet to be discovered. While there are a variety of experimental methods available to study protein-glycolipid binding *in vitro*, interpreting the binding data and relating them to the binding properties of protein-glycolipid interactions in a native membrane environment is generally not straightforward.<sup>6,7</sup>

Glycolipids, due to their amphipathic nature, can be readily immobilized on hydrophobic surfaces and their interactions with water-soluble carbohydrate binding proteins (lectins, antibodies and carbohydrate processing enzymes) can be probed using a variety of techniques, including enzyme-linked immunosorbent assays (ELISA), surface plasmon resonance (SPR) spectroscopy and thin layer chromatography (TLC) overlay.<sup>6</sup> Additionally, the use of glycolipid and neo-glycolipid microarrays enables the high-throughput screening of libraries of glycolipids.<sup>8-12</sup> These techniques can be applied to both natural and derivatized glycolipids and their application has led to the discovery of a number of protein-glycolipid receptors.<sup>13,14</sup> These aforementioned methods, however, all employ an artificial presentation of glycolipids and binding may be influenced by the nature of the coupling (immobilization) to the surface, ligand density, the loss of mobility of the glycolipid and effects related to the spatial orientation of the carbohydrate residues in the immobilized glycans.<sup>13</sup> Additionally, any required chemical modification of the protein or glycolipid, may influence the binding properties.<sup>8,15</sup>

Because the removal of glycolipids from a lipid environment is expected to influence the nature of protein interactions, extensive research efforts are being directed towards the development of

assays that allow protein-glycolipid binding to be studied under conditions where the glycolipid is maintained in a membrane environment.<sup>16</sup> To this end, the integration of a variety of model lipid bilayers with conventional biophysical binding assays have been reported. For example, protein binding to glycosphingolipids incorporated into supported phospholipid membranes, micelles (or glycomicelles) and liposomes (or glycoliposomes) has been studied using diverse spectroscopic methods (*e.g.*, fluorescence, nuclear magnetic resonance (NMR and SPR) and microscopy (*e.g.*, atomic force and total internal reflection fluorescence microscopy) techniques.<sup>16-22</sup> Recently, it was shown that the incorporation of glycosphingolipids into synthetic phospholipid bilayers called nanodiscs<sup>23-25</sup> enable protein-glycolipid binding to be studied in aqueous solution using a variety of analytical methods, including SPR spectroscopy,<sup>26</sup> electrospray ionization-mass spectrometry (ESI-MS)<sup>27,28</sup> and silicon photonic sensors.<sup>29</sup> While the use of these model lipid bilayers allow for the study of protein-glycolipid interactions in a membrane environment, there are challenges to accurately establishing and precisely controlling the size and composition of the bilayers.<sup>16</sup>

Here, we report on a new glycolipid presentation strategy which, in combination with state-of-the-art native ESI-MS, represents a significant contribution in the challenging area of protein-glycolipid interaction studies. The method exploits a naturally occurring lysosomal sphingolipid activator protein, saposin A (SapA), as a new and highly versatile approach for solubilizing glycolipids, while maintaining them in a lipid environment. SapA is a small (~9 kDa) alpha helical protein that binds to cellular lipids, including glycolipids, and transports them to lysosomal hydrolases for degradation as a small, soluble protein-lipid complex (~3 nm).<sup>30,31</sup> This lipid-transporting macromolecular complex, herein termed a *picodisc*, provides an ideal presentation environment for glycolipid hydrolysis. Indeed, saposins are essential to normal processing of lipids in the lysosome, and their dysfunction can result in lysosomal storage diseases.<sup>2</sup> Method validation

demonstrated that the plasma-membrane associated human neuraminidase (hNEU) enzyme, NEU3, can discriminate between ganglioside substrates (GM2 and GM3) within a picodisc.<sup>32</sup> Additionally, low, moderate and high affinity protein–glycolipid interactions were observed using picodiscs: Shiga toxin type 1 B subunit homopentamer binding with the globotriaosylceramide Gb3,<sup>33,34</sup> a monoclonal antibody-GD2 interaction,<sup>35</sup> and binding of the cholera toxin B subunit homopentamer (CTB<sub>5</sub>) with GM1.<sup>36</sup> Together, these data highlight the tremendous versatility of the picodisc/ESI-MS assay for protein–glycolipid interaction studies.

## **Experimental Section**

### **Proteins**

SapA (SapA) was expressed and purified as previously described.<sup>31</sup> Cholera toxin B subunit homopentamer from *Vibrio cholerae* (CTB<sub>5</sub>, 58020 Da) was purchased from Sigma-Aldrich Canada (Oakville, Canada) and the mouse monoclonal anti-GD2 antibody (clone 14.2Ga) from Millipore Canada Ltd. (Etobicoke, Canada). Shiga toxin type 1 B subunit homopentamer (Stx1B<sub>5</sub>, 38 455 Da) was a gift from Prof. G. Armstrong (University of Calgary). The human NEU3 (92 kDa) was expressed in BL21 (DE3) pLysS *Escherichia coli* cells as a MBP-fusion protein (pMAL-c2x vector). The protein was purified using an amylose affinity column (New England Biolabs) and its activity confirmed by through enzymatic reactions with a fluorogenic substrate, 2′-(4-methylumbelliferyl)- $\alpha$ -D-N-acetylneuraminic acid, as previously described.<sup>37</sup> The enzyme was stored in buffer containing 20 mM MOPs, 10 mM maltose, 10% glycerol, 0.3 M NaCl at -80 °C and buffer exchanged into 50 mM ammonium acetate pH 6.8 immediately prior to ESI-MS analysis.

### **Lipids**

1-palmitoyl-2-oleoyl-sn-glycero-3-phosphocholine (POPC) was purchased from Avanti Polar Lipids Inc. (Alabaster, AL). The gangliosides GM1 (1545.8 Da, 1573.9 Da) GM2 (1383.7 Da, 1411.7 Da)

and GM3 (1180.5 Da) were purchased from Enzo Life Science (Farmingdale, NY), and GD2 (1674.0 Da, 1702.0 Da) from MyBioSource Inc. (San Diego, CA). The globotriaosylceramide Gb3 was purchased from Abcam Inc. (Toronto, Canada).

### **Incorporation of glycolipids into picodiscs**

Picodiscs containing the scaffold protein, SapA, and the lipid, POPC, were chosen based on their previous characterization.<sup>31</sup> Picodiscs were prepared by mixing POPC and the glycolipid(s) of interest (dissolved in chloroform:methanol (2:1)) in a 1:4 ratio of glycolipid-to-POPC and the mixture dried under nitrogen gas to form a lipid film. Liposomes containing POPC and glycolipid were then formed by diluting the lipid film in 50 mM sodium acetate and 150 mM NaCl (pH 4.8) followed by a combination of sonication and freeze/thaw cycles. Picodisc formation was then initiated by the addition of SapA protein at 1:10 molar ratio of SapA to total lipid followed by incubation at 37 °C for 45 min. Finally, the picodiscs were purified using a Superdex 75 10/300 size-exclusion column (GE Healthcare Bio-Science, Uppsala, Sweden), equilibrated in 50 mM sodium acetate and 150 mM NaCl (pH 4.8). Control size-exclusion chromatography experiments in which liposomes containing POPC alone, POPC+GM1, POPC+GM2, POPC+GM3, POPC+GD2, POPC+Gb3 or SapA protein alone were individually injected onto the Superdex 75 10/300 column were carried out (Figures S1 and S2, Supporting Information). Immediately prior to ESI-MS analysis, the picodiscs were concentrated and buffer exchanged into 200 mM ammonium acetate (pH 6.8 for all binding studies and pH 4.8 for the enzymatic studies). The concentrations of glycolipid picodiscs were established from the concentration of SapA monomer, which was determined by the absorbance at 280 nm using an extinction coefficient of  $8855 \text{ M}^{-1} \text{ cm}^{-1}$ , and assuming a 1:1 ratio of ganglioside:SapA monomer.

### **Incorporation of glycolipids into nanodiscs**

Nanodiscs containing POPC and glycolipids were prepared as previously described.<sup>27,28</sup> Briefly, POPC (dissolved in chloroform: methanol at a 2:1 ratio) with GM2, GM3 or Gb3 were mixed together in a 99:1 ratio. The sample was dried under nitrogen and placed in a vacuum desiccator overnight to form a POPC lipid film. The membrane scaffold protein MSP1E1 was added to the lipid film at a molar ratio of 100:1 ratio of lipid to MSP1E1. The mixture was sonicated for 15 min in buffer containing 20 mM TrisHCl, 0.5 mM EDTA, 100 mM NaCl, and 25 mM sodium cholate at pH 7.4. After incubation for 15 min at 4 °C, the self-assembly process was initiated by adding pre-washed bio-beads (Bio-Rad Laboratories Ltd., Canada) and incubating for 3 h on an orbital shaker at 4 °C to remove all detergent. Finally, nanodiscs were purified using a Superdex 200 10/300 size exclusion column (GE Healthcare Bio-Science, Uppsala, Sweden) equilibrated in 200 mM ammonium acetate at pH 6.8. Nanodiscs were concentrated to approximately 20 µM and stored at -80 °C.

### **Electrospray ionization mass spectrometry analysis**

All ESI-MS measurements were carried out using a Synapt G2S instrument (Waters, Manchester, UK) equipped with a nano-ESI source. Negative ion mode was used for all the ESI-MS measurements involving ganglioside picodiscs (owing to the ease of detecting the deprotonated ganglioside ions); positive ion mode was used for the Gb3 containing picodiscs (released Gb3 was detected as the sodium adduct, i.e.,  $(Gb3 + Na)^+$ ). Borosilicate capillaries (1.0 mm o.d., 0.68 mm i.d.) were pulled in-house using a P-1000 micropipette puller (Sutter Instruments, Novato, CA). A platinum wire was inserted into the nanoESI tip and a capillary voltage of 0.8 kV (negative ion mode) or 1.0 kV (positive ion mode) was applied. For all experiments, a source temperature of 60 °C was used. For ESI-MS analysis of picodiscs, an argon gas flow of 2 mL min<sup>-1</sup> was used with the Trap and Transfer collision energies set to 5 and 2 V, respectively. Energy was applied in-source

(sampling cone voltage increased from 5 to 150 V) to dissociate the gaseous picodisc ions. Where necessary, the collision energy in the Trap region was increased using a Trap gas flow of 5 mL min<sup>-1</sup> to detect the released ganglioside ions.

For protein-glycolipid detection, optimization of the cone voltage was required for each sample; values used ranged from 30 to 150 V. To release glycolipids from the protein-complexes, the m/z region corresponding to the complex ions of interest was selected and subjected to CID in the Trap region using a collision energy of 50-100 V. The released ligands were identified based on the measured m/z of the corresponding ions. Where overlap between picodisc and protein-glycolipid complex occurred in the mass spectrum, CID was performed in the Transfer region using IMS to separate the protein-glycolipid complex from picodisc prior to CID.<sup>38</sup> For ion mobility spectrometry (IMS) measurements, which allowed for separation of the ions for the protein-glycolipid complexes and the picodiscs, a wave height of 40 V and a wave velocity of between 850 and 1000 m s<sup>-1</sup> was applied along with a helium and nitrogen (IMS gas) gas flow of 50 and 60 mL min<sup>-1</sup>, respectively. All data were processed using Mass Lynx software and, where applicable, Driftscope v.2.5 (Waters, Manchester, UK).

### **Enzymatic studies**

Enzymatic studies were performed by rapid manual mixing of NEU3 (0.0002 units) with picodiscs (10 μM ganglioside) or nanodiscs (10 μM ganglioside) in 200 mM ammonium acetate (pH 4.8). A 5 μL sample was then immediately injected into a nanoESI tip for time-resolved ESI-MS measurements, with data points measured at reaction times ranging from 5 to 80 min. To monitor the formation of sialic acid (SA) due to enzyme activity, GM3 and GM2 picodiscs or nanodiscs were incubated, separately, with NEU3. An internal standard, 5-acetamido-9-azido-3,5,9-trideoxy-D-glycero-D-galacto-2-nonulosonic acid (IS), synthesized as described by Cairo and co-workers,<sup>39</sup> was

added at a concentration of 2  $\mu\text{M}$ . The ion abundance (*Ab*) ratio of SA-to-IS was monitored as a function of reaction time (eq 1); each data point was calculated using summed ion abundances measured over a  $\pm 0.1$  min interval centred at the reaction time of interest. The ESI and instrumental voltages were: capillary 0.8–1.0 kV, cone 10 V and source offset 50 V. Control experiments, in which no enzyme was added to the disc solutions, were carried out to confirm that any SA detected was due to hydrolysis and not formed in the gas phase as a result of fragmentation of the GM3 or GM2 in the picodiscs or nanodiscs.

$$\text{SA/IS} = \text{Ab}(\text{SA})/\text{Ab}(\text{IS}) \quad (1)$$

To monitor the depletion of substrate from the picodiscs/nanodiscs, GM2 picodiscs/nanodiscs and GM3 picodiscs/nanodiscs were mixed in a 1:1 ratio. The *Ab* ratios of GM2 and GM3 ions, relative to SapA ions (eqs 2 and 3), released from the picodiscs by CID were measured over time. To dissociate the gas-phase picodisc/nanodisc ions, sampling cone voltages of 110 and 150 V, respectively, and Trap collision energies of 50 and 150 V, respectively, were used; the Trap gas flow rate was 8 mL min<sup>-1</sup>. All other instrumental parameters were the same as those used for the SA detection measurements. In all cases, the pH of the solution prior to the addition of enzyme and after the enzymatic reaction was directly measured to confirm no pH change had occurred.

$$\text{GM2/SapA} = \text{Ab}(\text{GM2})/\text{Ab}(\text{SapA}) \quad (2)$$

$$\text{GM3/SapA} = \text{Ab}(\text{GM3})/\text{Ab}(\text{SapA}) \quad (3)$$

### **Protein-glycolipid complex formation**

CTB<sub>5</sub> (20  $\mu\text{M}$ ) was mixed with GM1 picodiscs (44  $\mu\text{M}$  ganglioside), anti-GD2 antibody (1.5  $\mu\text{M}$ ) with GD2 picodiscs (50  $\mu\text{M}$  ganglioside), Stx1B<sub>5</sub> (8  $\mu\text{M}$ ) with Gb3 picodiscs (47  $\mu\text{M}$  Gb3) and Stx1B<sub>5</sub> (8  $\mu\text{M}$ ) with Gb3 nanodiscs (47  $\mu\text{M}$  Gb3) in 200 mM ammonium acetate (pH 6.8). After 5

min incubation at room temperature, the mixtures were loaded into the ESI tip and mass spectra acquired. Mass spectra acquired ~5 min after mixing and 1 hr after mixing confirmed the binding equilibrium had been reached after 5 min of incubation in all cases.

### Direct ESI-MS assay

The direct ESI-MS assay<sup>40</sup> was used to measure the apparent association constants ( $K_{a,app}$ ) for the binding of the oligosaccharide GD2<sub>os</sub> to anti-GD2 mouse mAb. Prior to analysis, the mAb solution was diluted in 200 mM ammonium acetate (pH 6.8) and concentrated using Amicon Ultra-4 centrifugal filters with a molecular weight cut-off 100,000 Da. Each ESI solution was prepared from stock solutions of protein and oligosaccharide. A minimum of five different initial ligand concentrations was used for each oligosaccharide tested and the binding measurements were carried out in triplicate. A complete description of the data analysis method employed to calculate the association constants ( $K_a$ ) can be found elsewhere<sup>40</sup> and only a brief overview is given here. Briefly, the abundance ratio ( $R_i$ ) of the protein bound to  $i$  molecules of L ( $PL_i$ ) to free protein (P) measured by ESI-MS (after correction for nonspecific ligand-protein binding) is taken to be equal to the equilibrium concentration ratio in solution, eq 4:

$$R_i = \frac{\sum Ab(PL_i)}{\sum Ab(P)} = \frac{[PL_i]}{[P]} \quad (4)$$

and the apparent association constant ( $K_{a,i}$ ) for the addition of the  $i^{th}$  L to P bound to  $(i-1)L$  can be expressed by eq 5:

$$K_{a,i} = \frac{R_i / R_{i-1}}{[P]_0 \sum_{i=1}^h i R_i} \quad (5)$$

$$[L]_0 - \frac{i=1}{h} \frac{1}{1 + \sum_{i=1}^h R_i}$$

where  $h$  is the number of ligand binding sites and  $[P]_0$  and  $[L]_0$  are the initial concentrations of the protein and ligand, respectively. Expressions for the apparent  $K_{a,i}$  values for the stepwise binding of one and two ligand molecules, i.e.,  $K_{a,1}$  and  $K_{a,2}$ , to the mAb are given by eqs 6 and 7:

$$K_{a,1} = \frac{R_1}{[L]_0 - \frac{(R_1 + 2R_2)[P]_0}{1 + R_1 + R_2}} \quad (6)$$

$$K_{a,2} = \frac{R_2}{R_1 \left( [L]_0 - \frac{(R_1 + 2R_2)[P]_0}{1 + R_1 + R_2} \right)} \quad (7)$$

## Results and Discussion

### a. Incorporation of glycolipids into picodiscs

Glycolipid-containing picodiscs were formed *in vitro* through incubation of POPC liposomes containing glycolipid with SapA protein. Consistent with previous results obtained for galactosylceramide-containing picodiscs, size exclusion chromatography suggested the presence of a 35 kDa complex (Figures S1 and S2, Supporting Information).<sup>31</sup> ESI-MS analysis of aqueous solutions of picodiscs failed to detect the presence of free glycolipid (Figure S3, Supporting Information). Moreover, collision-induced dissociation (CID) performed on the gaseous picodisc ions revealed the loss of deprotonated glycolipid in all cases (Figure S4, Supporting Information). Together, these results confirm the successful incorporation of glycolipids into the discs.

### b. Picodiscs present glycolipids for enzymatic processing

Validation of picodiscs as a means of presenting glycolipids for enzymatic studies in aqueous solution was carried using reactions involving the plasma-membrane associated hNEU, NEU3, and ganglioside substrates GM2 and GM3.<sup>32</sup> NEU3 can cleave sialic acid (SA) from GM2 and GM3 (Figure S5, Supporting Information) and is known to be more active against GM3.<sup>41,42</sup> Picodiscs

containing either GM2 or GM3 were incubated with NEU3 in 200 mM ammonium acetate (pH 4.8 and 22 °C) and the abundance of the singly deprotonated ion of SA was monitored in real-time with ESI-MS and compared to an internal standard (IS) (Figure S5, Supporting Information). As expected based on the greater activity of NEU3 for GM3, as compared with GM2,<sup>41</sup> SA release by NEU3 was readily observed with the GM3 picodiscs (Figure 1a), whereas little free SA was observed in the case of the GM2 picodiscs (Figure 1b). Although SA is generated by enzyme cleavage of both GM2 and GM3, it is possible to monitor the rate of desialylation of both gangliosides, simultaneously, by dissociating the picodisc ions in the gas phase using CID. Analysis of NEU3 with picodiscs containing an equimolar mixture of GM2 and GM3 in ESI-CID-MS measurements allowed the relative abundances of the GM2 and GM3 substrates to be monitored over time (Figure 1c). Consistent with the results obtained for the formation of SA in picodiscs with a single ganglioside, the abundance of GM3 decreased with reaction time relative to GM2. Control experiments, performed in the absence of NEU3, showed that the abundance ratio of GM3 and GM2 ions remains constant over this time period and confirm that the picodiscs remain intact (Figure S6, Supporting Information). Comparison of the relative abundances of intact GM2 and GM3 (monitored as the abundance ratios of GMX to released SapA ions) with those measured for SA from the individual GM2 or GM3 picodiscs (monitored as the abundance ratio of SA/IS) shows that the decrease in substrate abundance correlates with the increase in SA formation (Figure 1d). Notably, when incorporated into a nanodisc containing POPC, GM3 exhibits no measurable reactivity with NEU3 under similar experimental conditions (Figure S7, Supporting Information).

These findings suggest that picodiscs, consistent with their hypothesized role in glycolipid degradation, allow for a more native-like presentation of glycolipids for enzymatic studies compared to model lipid bilayers. The use of picodiscs in ESI-MS analysis requires no synthetic modification

of the glycolipid and should require less material than TLC-based assays. Taken together, these results illustrate the tremendous opportunity afforded by glycolipid-loaded picodiscs, combined with real-time ESI-MS analysis, for studying the enzymatic degradation of glycolipids, which are key regulators in diabetes, cancer, and cellular adhesion.<sup>43</sup>

### **c. Picodiscs for antibody-antigen interaction analysis**

Antibodies represent an important class of therapeutics due to their ability to recognize “undruggable” targets.<sup>44</sup> Here, we demonstrate the application of picodiscs as a means of presenting glycolipids for mAb binding studies. Picodiscs containing GD2 (50  $\mu$ M) (in a 1:1:4 SapA:GD2:POPC ratio) were incubated with an anti-GD2 mouse mAb (1.5  $\mu$ M) in 200 mM aqueous ammonium acetate (pH 6.8, 22 °C) and mAb-GD2 interactions monitored by ESI-MS. Signal consistent (in terms of mass-to-charge ratio ( $m/z$ )) with free mAb ions, as well as mAb with one and two GD2 molecules, was detected (Figure 2a). Upon CID of ions in an  $m/z$  window centered at 6923, which corresponds to the -22 charge state of the (mAb + 2GD2) complex, singly and doubly deprotonated GD2 ions were detected, along with free mAb and mAb with one GD2 molecule bound, confirming the binding of GD2 to the mAb (Figure S8, Supporting Information). From the relative abundances of free and GD2-bound mAb species measured by ESI-MS, the apparent affinities of GD2 picodiscs for the stepwise binding to the two mAb binding sites were estimated ( $K_{a1} = 5 \times 10^4 \text{ M}^{-1}$ ,  $K_{a2} = 2 \times 10^4 \text{ M}^{-1}$ ). In separate experiments, the affinities of the GD2 oligosaccharide (GD2<sub>os</sub>) for the mAb were found ( $K_{a1} = 6 \times 10^4 \text{ M}^{-1}$ ,  $K_{a2} = 3 \times 10^4 \text{ M}^{-1}$ ) using the direct ESI-MS assay. The similarity in the measured values suggests that, in this case, the ceramide moiety does not significantly influence the recognition of the GD2 antigen by the mAb.

### **d. Picodiscs for bacterial toxin-glycolipid interaction analysis**

The interaction between CTB<sub>5</sub> and GM1 has been extensively studied and serves as a model for protein-glycosphingolipid binding. The B subunit homopentamer can bind up to five molecules of GM1, with relatively high affinity.<sup>36</sup> Stepwise binding of the GM1 pentasaccharide to CTB<sub>5</sub> exhibits positive cooperativity with intrinsic (per binding site) affinities ranging from 10<sup>5</sup> to 10<sup>6</sup> M<sup>-1</sup>.<sup>45</sup> ESI-MS analysis of an aqueous solution of CTB<sub>5</sub> and GM1 picodiscs (in a 1:1:4 SapA:GM1:POPC ratio) in 200 mM aqueous ammonium acetate (pH 6.8, 22 °C) produced signal corresponding to the -15 to -18 charge states of CTB<sub>5</sub> bound to four or five GM1 molecules, in addition to ions in the 3000-4500 m/z range, which correspond to GM1 picodisc (Figure 2b). CID performed on the (CTB<sub>5</sub> + 5GM1) complex, at the -16 charge state (m/z window centered at 4117), resulted in the appearance of both CTB monomer and GM1 ions, in addition to ions corresponding to SapA with 0-4 POPC molecules bound (Figure S9, Supporting Information). The appearance of the SapA ions is due to the mass spectral overlap for the corresponding gas-phase ions of the CTB<sub>5</sub> complexes and the picodiscs. However, using ion mobility spectrometry (IMS), which separates gaseous ions based on their charge and shape,<sup>46</sup> complete separation of the ions corresponding to the (CTB<sub>5</sub> + 4GM1) and (CTB<sub>5</sub> + 5GM1) complexes and those of the GM1 picodisc ions was achieved (Figure 3).

To demonstrate the utility of the newly developed picodiscs/ESI-MS assay for detecting low affinity protein-glycolipid binding, it was applied to the interaction between Shiga toxin type 1 (Stx1) and its native globotriaosylceramide receptor Gb3.<sup>33,34</sup> The intrinsic K<sub>a</sub> for the binding of the trisaccharide of Gb3 to the highest affinity sites of the Stx1 B subunit homopentamer (Stx1B<sub>5</sub>) is reported to be (0.27 ± 0.08) × 10<sup>3</sup> M<sup>-1</sup>.<sup>47</sup> ESI-MS analysis of an aqueous solution of Stx1B<sub>5</sub> (8 μM) and Gb3 picodiscs (47 μM, in a 1:1:4 SapA:Gb3:POPC ratio) in 200 mM aqueous ammonium acetate (pH 6.8, 22 °C) produced signal corresponding to the +12 to +15 charge states of free Stx1B<sub>5</sub> and Stx1B<sub>5</sub> bound to one Gb3 ligand (Figure 4a). CID was used to further confirm the identity of the

(Stx1B<sub>5</sub> + Gb3) complex. Following isolation of a narrow m/z window centered at 3044, which corresponds to the +13 charge state of the (Stx1B<sub>5</sub> + Gb3) complex, CID resulted in the appearance of free B subunits ions, as well as the (Gb3 + Na)<sup>+</sup> ion (Figure 4b). From the relative abundances of free and Gb3-bound Stx1B<sub>5</sub> ions, the intrinsic affinity of the Gb3 picodiscs for Stx1B<sub>5</sub> was estimated to be 0.2×10<sup>3</sup> M<sup>-1</sup>, which is close agreement with reported affinity for the Gb3 trisaccharide. Notably, ESI-MS measurements carried out on an aqueous solution of Stx1B<sub>5</sub> (8 μM) and POPC nanodiscs containing 1% Gb3 (47 μM Gb3) in 200 mM aqueous ammonium acetate (pH 6.8, 22 °C) failed to produce detectable signal corresponding to the Gb3-bound Stx1B<sub>5</sub> (Figure S10, Supporting Information). These results suggest that picodiscs may offer advantages over nanodiscs in the detection of low affinity protein-glycolipid interactions.

## Conclusions

In summary, we have developed a powerful new method, which combines picodiscs and native ESI-MS, for protein-glycolipid interaction analysis *in vitro*. The results of time-resolved measurements of enzyme-catalysed hydrolysis of glycolipid substrates and the detection of known high, moderate and low-affinity protein-glycolipid interactions demonstrate the reliability and versatility of the picodisc/ESI-MS assay. Finally, it should be noted that, although ESI-MS was the method of detection employed in the current study, the picodiscs represent a general strategy for solubilizing glycolipids for biological investigation studies and could be incorporate into a variety of other biophysical techniques, including SPR spectroscopy, ELISA and glycolipid microarrays.

## ASSOCIATED CONTENT

### Supporting Information

Mass spectra, chromatograms and structures. This material is available free of charge via the Internet at <http://pubs.acs.org>.

**Author Information****Corresponding Author**

john.klassen@ualberta.ca

**Notes**

The authors declare no competing financial interests.

**Acknowledgment**

The authors are grateful for financial support provided by the National Sciences and Research Council of Canada and the Alberta Glycomics Centre (J.S.K. and C.W.C.) and the Canadian Institutes of Health Research (G.G.P.).

## References

1. Varki, A.; Cummings, R.D.; Esko, J.D.; Freeze, H.H.; Stanley, P.; Bertozzi, C.R.; Hart, G.W.; Etzler, M.E. *Essentials of Glycobiology* 2nd Ed. Cold Spring Harbor Laboratory Press, Cold Spring Harbor, New York, USA 2009.
2. Schulze, H.; Sandhoff, K. *Biochim Biophys Acta*. **2014**, *1841*, 799.
3. Meyer, S.; van Liempt, E.; Imberty, A.; van Kooyk, Y.; Geyer, H.; Geyer, R.; van Die, I. *J Biol Chem*. **2005**, *280*, 37349.
4. Janes, P.W.; Ley, S.C.; Magee, A.I.; Kabouridis, P.S. *Semin Immunol*. **2000**, *12*, 23.
5. Yamamoto, M.; Boyer, A.M.; Schwarting, G.A. *Proc Natl Acad Sci U S A*. **1985**, *82*, 3045.
6. Lopez P.H.; Schnaar, R.L. *Methods Enzymol*. **2006**, *417*, 205.
7. Lipid-Protein Interactions. Kleinschmidt, J.H. Ed.; in *Methods and Protocols*, 974, Springer: New York, 2014.
8. Song, X.; Heimburg-Molinaro, J.; Cummings, R.D.; Smith, D.F. *Curr. Opin. Chem. Biol.* **2014**, *18*, 70.
9. Feizi T. *Ann N Y Acad Sci*. **2013**, *1292*, 33.
10. Palma, A.S.; Feizi T, Childs RA, Chai W, Liu Y. *Curr Opin Chem Biol*. **2014**, *18*, 87.
11. Rinaldi, S.; Brennan, K.M.; Goodyear, C.S.; O'Leary, C.; Schiavo, G.; Crocker, P.R.; Willison, H.J. *Glycobiology* **2009**, *19*, 789.
12. Arigi, E.; Blixt, O.; Buschard, K.; Clausen, H.; Lavery, S.B. *Glycoconj. J*. **2012**, *1*, 1.
13. Grant, OC, Smith, HM, Firsova, D, Fadda, E, Woods, RJ. *Glycobiology* **2014**, *24*, 17.
14. Campanero-Rhodes, M.A.; Smith, A.; Chai, W.; Sonnino, S.; Mauri, L.; Childs, R.A.; Zhang, Y.; Ewers, H.; Helenius, A.; Imberty, A.; Feizi, T. *J. Virol*. **2007**, *81*, 12846.
15. Stowell, S.R.; Arthur, C.M.; Mehta, P.; Slanina, K.A.; Blixt, O.; Leffler, H.; Smith, D.F.; Cummings, R.D. *J. Biol. Chem*. **2008**, *283*, 10109.

16. Czogalla A., Grzybek M., Jones W., Coskun U. *Biochim. Biophys. Acta.* **2014**, *1841*, 1049.
17. Cho, H.; Wu, M.; Bilgin, B.; Walton, S.P.; Chan, C. *Proteomics* **2012**, *12*, 3273.
18. Sanghera, N.; Correia, B.E.; Correia, J.R.; Ludwig, C.; Agarwal, S.; Nakamura, H.K.; Kuwata, K.; Samain, E.; Gill, A.C.; Bonev, B.B.; Pinheiro, T.J. *Chem. Biol.* **2011**, *18*, 1422.
19. Shi, J.; Yang, T.; Kataoka, S.; Zhang, Y.; Diaz, A.J.; Cremer, P.S. *J. Am. Chem. Soc.* **2007**, *129*, 5954-5961.
20. Rao CS., Lin X, Pike HM, Molotkovsky JG, Brown RE. *Biochemistry* **2004**, *43*, 13805-13815.
21. Chen, W.C.; Kawasaki, N.; Nycholat, C.M.; Han, S.; Pilotte, J.; Crocker, P.R.; Paulson, J.C. *PLoS One* **2012**, *7*, e39039.
22. Jayaraman, N.; Maiti, K.; Naresh, K. *Chem. Soc. Rev.* 2013, *42*, 4640-4656.
23. Nath, A.; Atkins, W.M.; Sligar, S.G. *Biochemistry* **2007**, *46*, 2059-2069.
24. Bayburt, T.H.; Sligar, S.G. *FEBS Letters* **2010**, *584*, 1721-1727.
25. Denisov, I.G.; Grinkova, Y.V.; Lazarides, A.A.; Sligar, S.G. *J. Am. Chem. Soc.* **2004**, *126*, 3477.
26. Borch, J.; Torta, F.; Sligar, S.G.; Roepstorff, P. *Anal. Chem.* **2008**, *80*, 6245.
27. Zhang, Y.; Liu, L.; Daneshfar, R.; Kitova, E.N.; Li, C.; Jia, F.; Cairo, C.W.; Klassen, J.S. *Anal. Chem.* **2012**, *84*, 7618.
28. Leney, A.; Fan, X.; Kitova, E.N.; Klassen, J.S. *Anal. Chem.* **2014**, *86*, 5271.
29. Sloan, C.D.K.; Marty, M.T.; Sligar, S.G.; Bailey, R.C. *Anal. Chem.* **2013**, *85*, 2970.
30. Locatelli-Hoops, S.; Rimmel, N.; Klingenstein, R.; Breiden, B.; Rossocha, M.; Schoeniger, M.; Koenigs, C.; Saenger, W.; Sandhoff, K.. *J Biol Chem.* **2006**, *281*, 32451.
31. Popovic, K.; Holyoake, J.; Pomès, R.; Privé, G.G. *Prot. Nat. Acad. Sci.* **2012**, *109*, 2908.

32. Cairo, C.W. *Med. Chem. Commun.* **2014**, *5*, 1067.
33. Lingwood, C.A.; Law, H.; Richardson, S.; Petric, M.; Brunton, J.L.; De Grandis, S.; Karmali, M. *J. Biol. Chem.* **1987**, *262*, 8834.
34. Paton, J.C.; Paton, A.W. *Clin. Microbiol. Rev.* **1998**, *11*, 450.
35. Mujoo, K.; Kipps, T.J.; Yang, H.M.; Cheresch, D.A.; Wargalla, U.; Sander, D.J.; Reisfeld, R.A. *Cancer Res.* **1989**, *49*, 2857.
36. Holmgren, J.; Lönnroth, I.; Svennerholm, L. *Infect. Immun.* **1973**, *8*, 208.
37. Albohy, A., Li, M.D., Zheng, R.B., Zou, C., Cairo, C.W. *Glycobiology* **2010**, *20*, 1127.
38. Shepherd, D.A.; Marty, M.T.; Giles, K.; Baldwin, A.T.; Benesch, J.L.P. *Int. J. Mass spectrom.* in press.
39. Sandbhor, M.S.; Soya, N.; Albohy, A.; Zheng, R.B.; Cartmell, J.; Bundle, D.R.; Klassen, J.S.; Cairo, C.W. *Biochemistry* **2011**, *50*, 6753.
40. Kitova, E. N.; El-Hawiet, A.; Schnier, P. D.; Klassen, J. S. *J. Am. Soc. Mass Spectrom.* **2012**, *23*, 431.
41. Ha, K., Lee, Y., Cho, S., Kim, J., Kim, C. *Mol. Cells* **2003**, *17*, 267.
42. Li, S.C.; Li, Y.T.; Moriya, S.; Miyagi, T. *Biochem. J.* **2001**, *360*, 233.
43. Miyagi, T.; Yamaguchi, K. *Glycobiology* **2012**, *22*, 880.
44. Chames, P.; Regenmortel, M.V.; Weiss, E.; Baty, D. *Br. J. Pharmacol.* **2009**, *157*, 220.
45. Lin, H.; Kitova, E.N.; Klassen, J.S. *J. Am. Soc. Mass Spectrom.* **2014**, *25*, 104.
46. Hoaglund, C.S.; Valentine, S.J.; Sporleder, C.R.; Reilly, J.P.; Clemmer, D.E. *Anal. Chem.* **1998**, *70*, 2236.
47. Sun, J.; Kitova, E.N.; Wang, W.; Klassen, J.S. *Anal. Chem.* **2006**, *78*, 3010.

## Figure Captions

**Figure 1.** Enzymatic hydrolysis of gangliosides. Time-resolved ESI-MS analysis of 200 mM aqueous ammonium acetate solutions (pH 4.8, 22 °C) containing NEU3 and (a) GM3 picodiscs (10 μM ganglioside) or (b) GM2 picodiscs (10 μM ganglioside), with 2 μM internal standard (IS). Signal corresponding to maltose, which is present in the NEU3 stock solution, indicated by \*. (c) Time-resolved ESI-CID-MS of picodisc ions produced from a 1:1 mixture of GM2 and GM3 picodiscs (10 μM ganglioside) in a 200 mM aqueous ammonium acetate solution (pH 4.8, 22 °C) with NEU3. (d) Plots of SA:IS abundance ratios measured for GM2 picodiscs (blue) and GM3 picodiscs (red), and GMX/SapA (where GMX = GM2 or GM3) abundance ratios measured for a 1:1 mixture of GM2 and GM3 picodiscs.

**Figure 2.** Protein-glycolipid binding studies using ganglioside-containing picodiscs. ESI-MS analysis of 200 mM aqueous ammonium acetate solutions (pH 6.8, 22 °C) containing (a) anti-GD2 mAb (1.5 μM) with GD2 picodiscs (50 μM ganglioside) or (b) CTB<sub>5</sub> (20 μM) with GM1 picodiscs (44 μM ganglioside).

**Figure 3.** (a) Intensity map of m/z versus IMS arrival times measured for ions produced by ESI performed on an aqueous ammonium acetate solution (200 mM, pH 6.8) of CTB<sub>5</sub> (20 μM) and GM1 picodisc (44 μM). Mass spectra of the ions corresponding to (b) (CTB<sub>5</sub> + 5GM1) and (CTB<sub>5</sub> + 4GM1) complexes and (c) the picodiscs extracted using Driftscope (v.2.5).

**Figure 4.** (a) ESI-MS analysis of a 200 mM aqueous ammonium acetate solution (pH 6.8, 22 °C) containing Stx1B<sub>5</sub> (8 μM) with Gb3 picodiscs (47 μM Gb3). (b) CID mass spectrum acquired for the (Stx1B<sub>5</sub> + Gb3)<sup>13+</sup> ion.

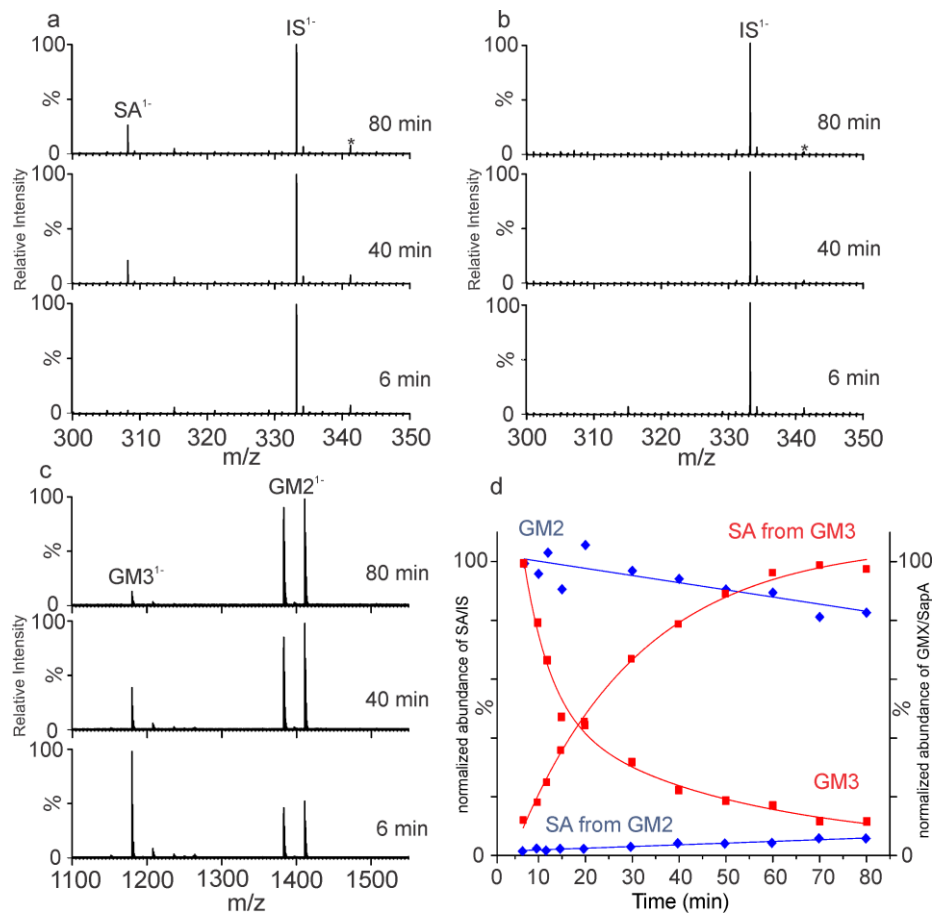


**Figure 1**

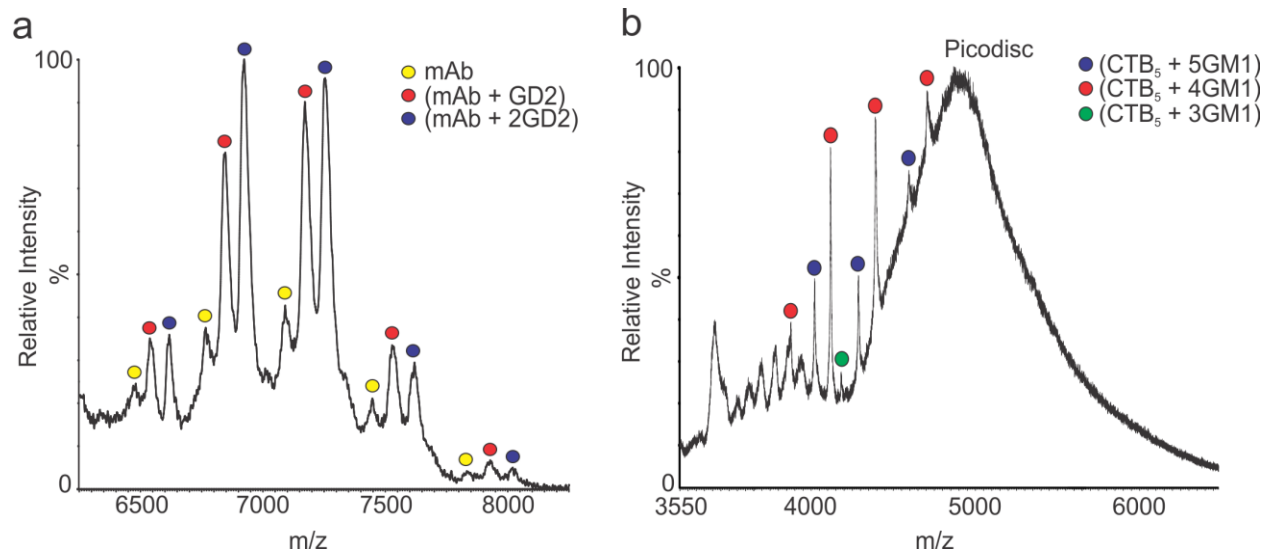


**Figure 2**

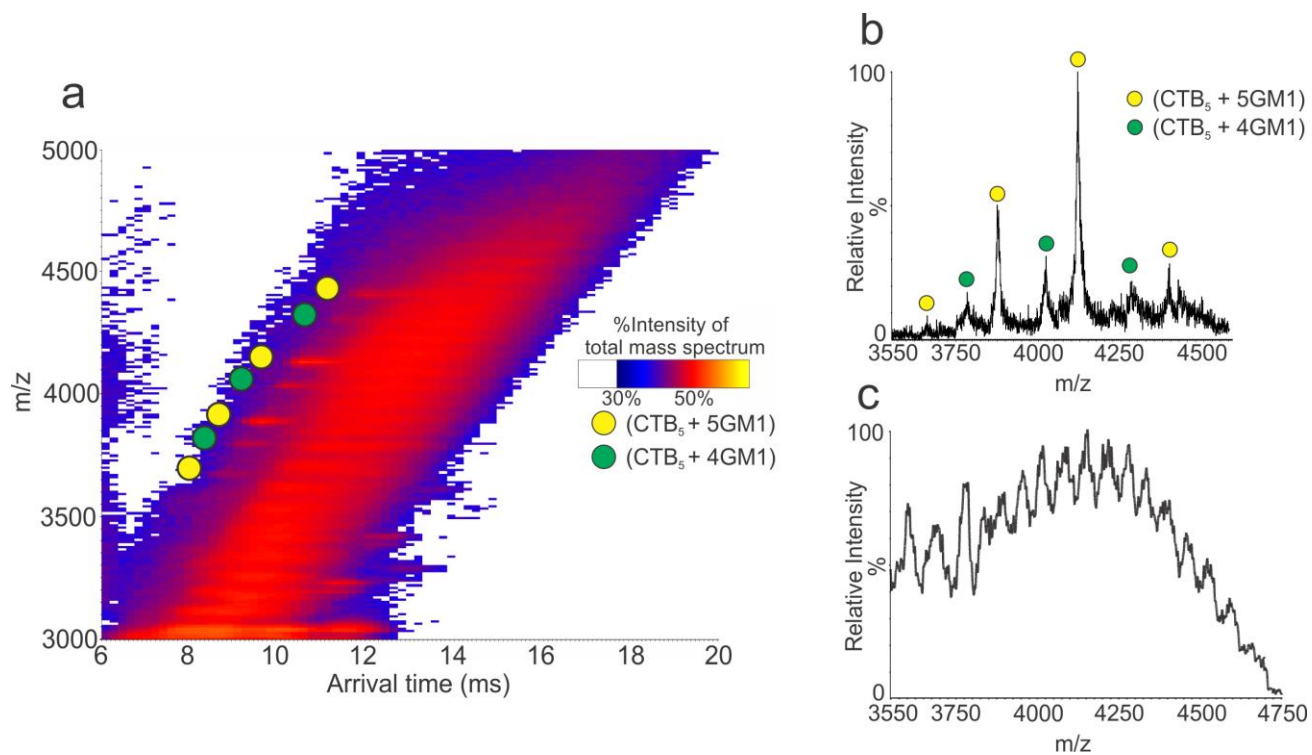


**Figure 3**

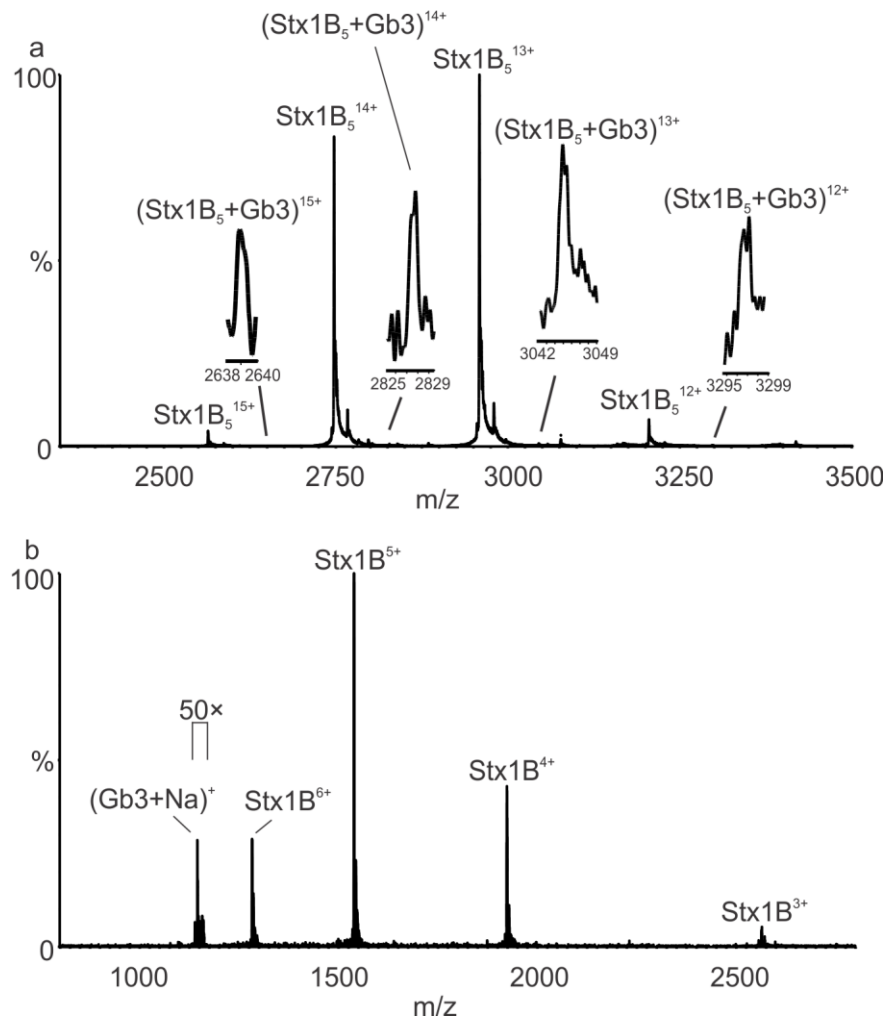
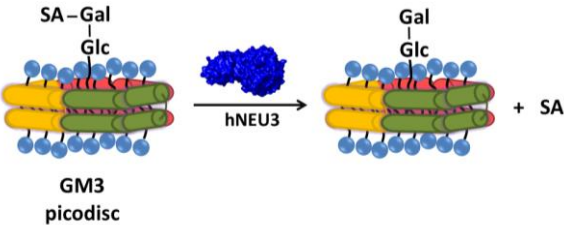


**Figure 4**

TOC graphic



## SUPPLEMENTARY INFORMATION FOR:

### Picodiscs Display Glycolipids for Facile ESI-MS Analysis of Protein Interactions

Aneika C. Leney, Reza Rezaei Darestani, Jun Li, Sanaz Nikjah, Elena N. Kitova, Chunxia Zou,

Christopher W. Cairo, Zi Jian Xiong, Gilbert G. Privé and John S. Klassen

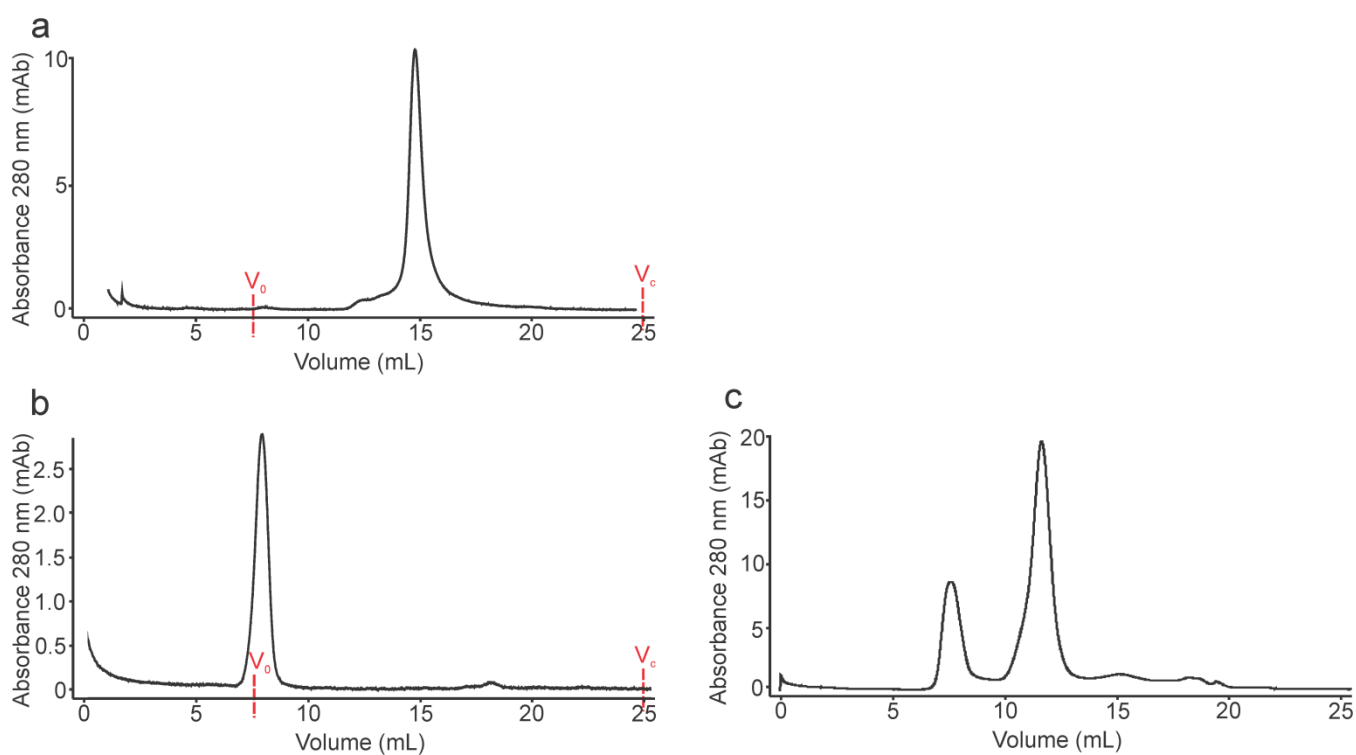


**Fig. S1.** Size exclusion chromatography of (a) SapA alone (no lipid), (b) POPC liposomes, (c) POPC liposomes with SapA. Liposomes and SapA elute at volumes of ~7 mL and ~15 mL, respectively, while the picodiscs elute at a volume of ~11.5 mL.

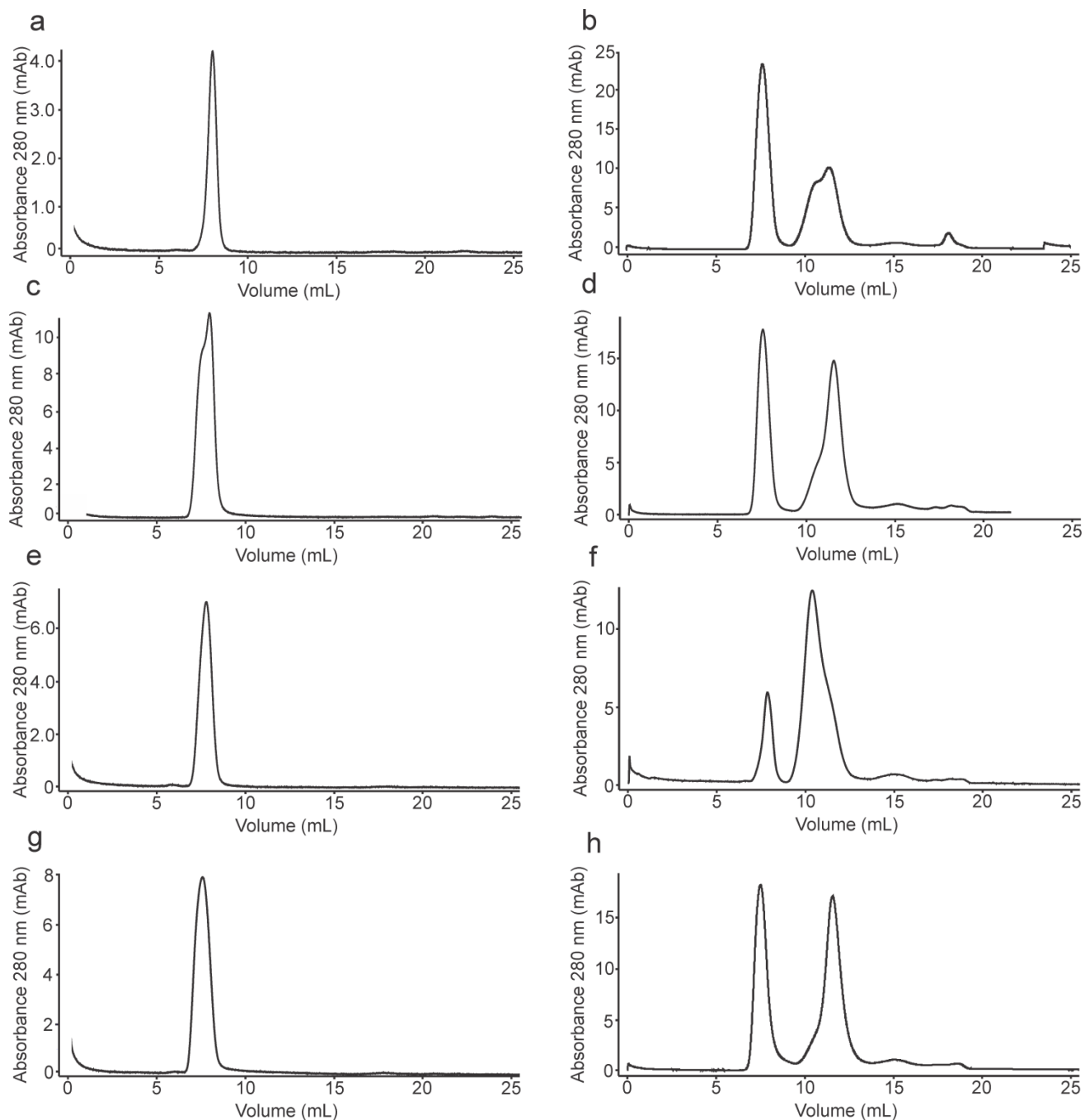


**Fig. S2.** Size exclusion chromatography of (a) POPC/GM1 liposomes, (b) POPC/GM1 liposomes with SapA, (c) POPC/GM2 liposomes, (d) POPC/GM2 liposomes with SapA, (e) POPC/GM3 liposomes, (f) POPC/GM3 liposomes with SapA, (g) POPC/GD2 liposomes, (h) POPC/GD2 liposomes with SapA. SapA picodiscs in samples b, d, f and h corresponding to an elution volume of ~11.5 mL were collected for subsequent ESI-MS analysis.

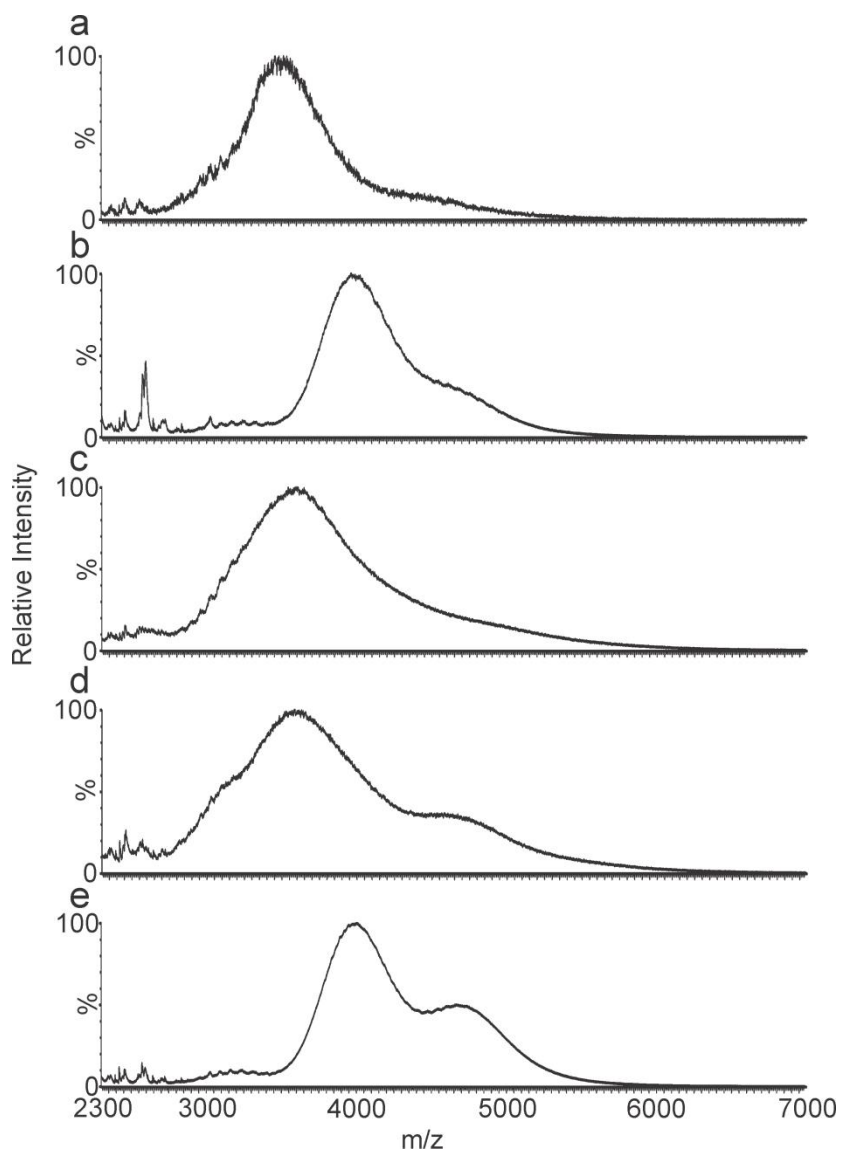


**Fig. S3.** ESI-MS analysis of (a) empty (POPC only) picodiscs at pH 4.8, and picodiscs containing (b) GM1 at pH 6.8, (c) GM2 at pH 4.8, (d) GM3 at pH 4.8, and (e) GD2 at pH 6.8.

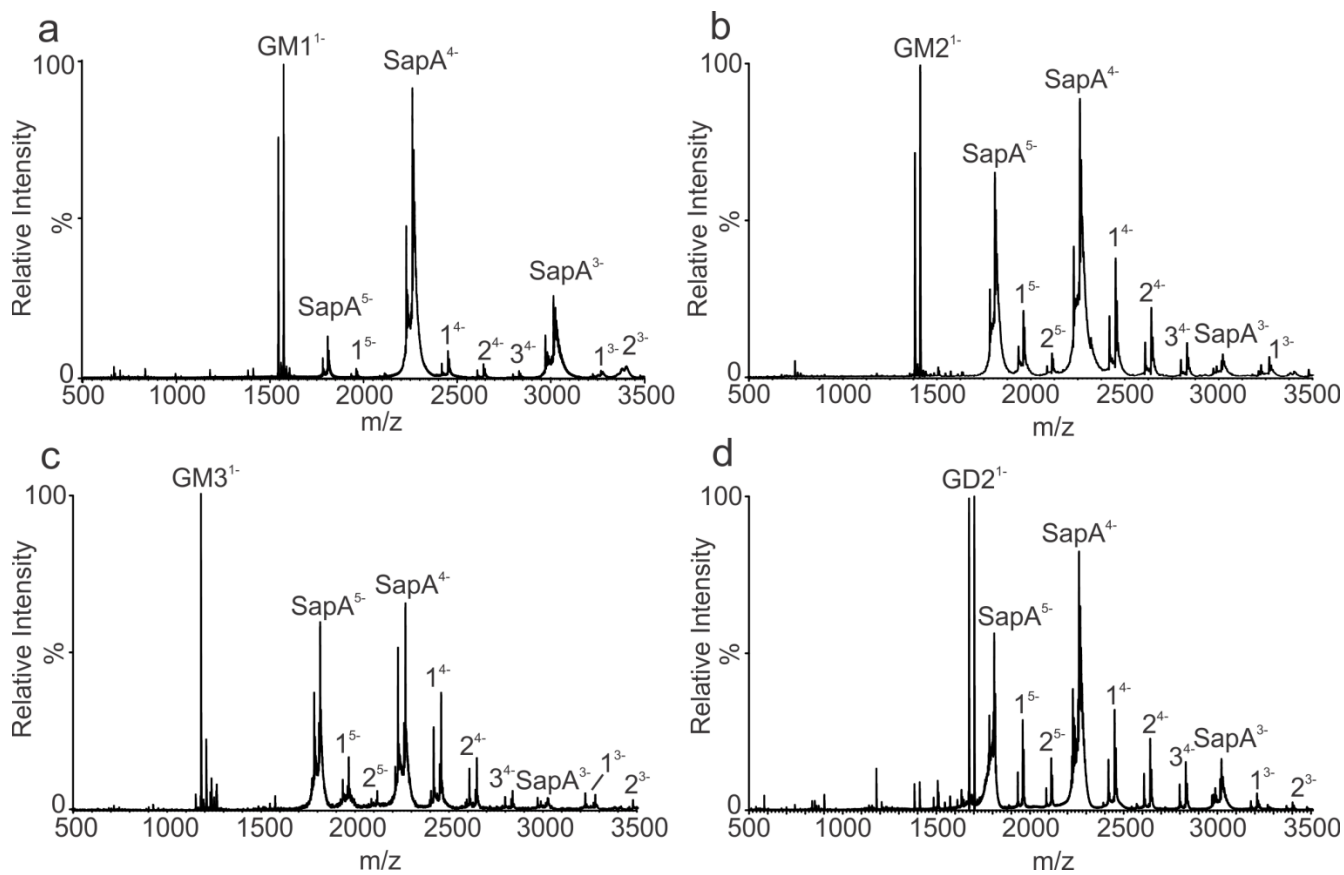


**Fig. S4.** CID mass spectra of ganglioside picodisc ions produced by ESI performed on aqueous ammonium acetate solutions (200 mM, pH 6.8). CID was carried out in the Trap region using collision energies of 30 - 100 V. (a) GM1, (b) GM2, (c) GM3 and (d) GD2. Peaks labelled 1, 2 and 3 correspond to SapA-POPC complexes with 1, 2 and 3 POPC molecules bound, respectively.

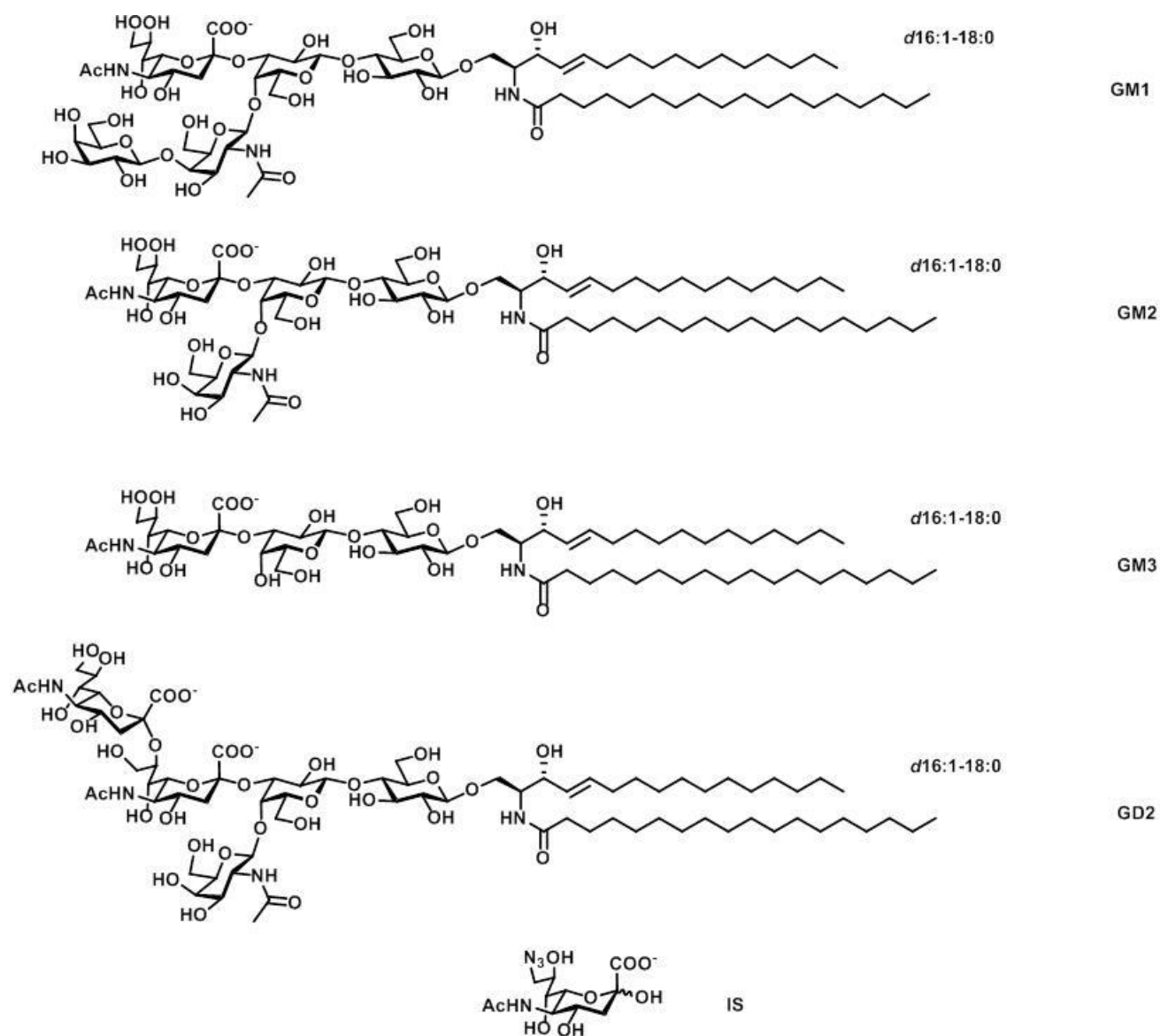


**Fig. S5.** Structures of gangliosides GM1, GM2, GM3 and GD2 and 5-acetamido-9-azido-3,5,9-trideoxy-D-glycero-D-galacto-2-nonulosonic acid (IS), which served as an internal standard for the enzyme kinetics assay.

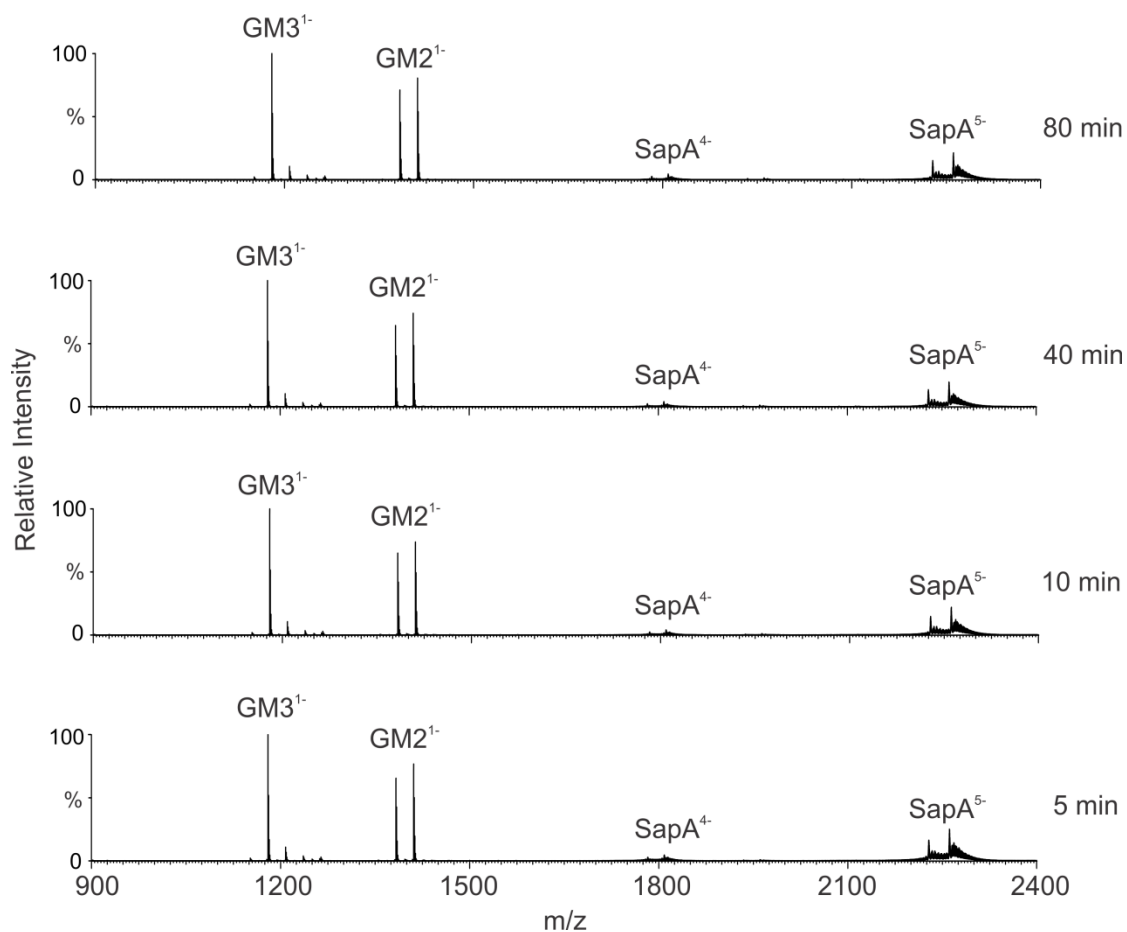


**Fig. S6.** CID mass spectra of GM2 picodiscs and GM3 picodiscs produced by ESI performed on aqueous ammonium acetate solutions (200 mM, pH 4.8) at (a) 5 min, (b) 10 min, (c) 40 min and (d) 80 min after mixing. CID was carried out in the Trap region using a collision energy of 50 V.

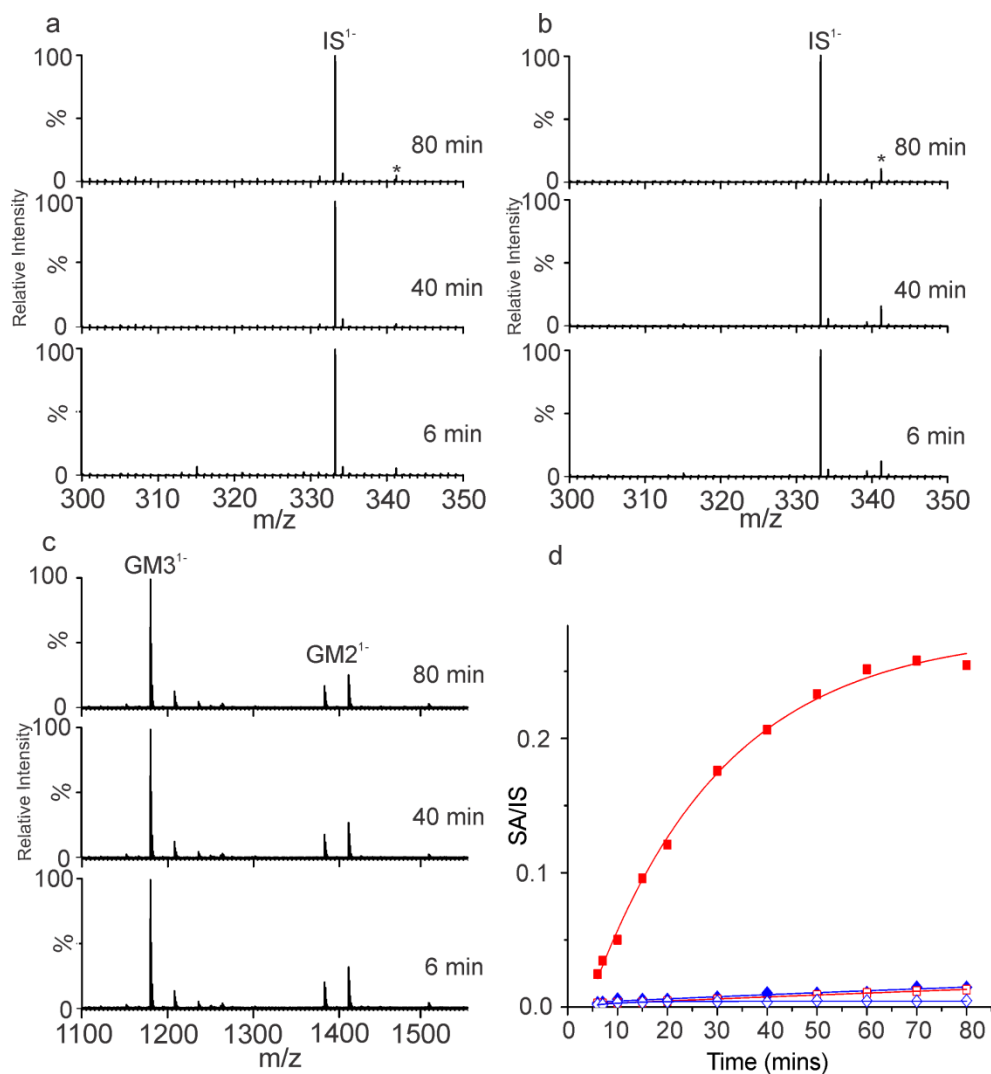


**Fig. S7.** Enzymatic hydrolysis of gangliosides in picodiscs and nanodiscs. Time-resolved ESI-MS analysis of 200 mM aqueous ammonium acetate solution (pH 4.8, 22 °C) containing hNeu3 and (a) GM3 nanodiscs (10  $\mu$ M ganglioside) or (b) GM2 nanodiscs (10  $\mu$ M ganglioside), and 2  $\mu$ M internal standard (IS). Signal corresponding to maltose, which is present in the hNeu3 stock solution, indicated by \*. (c) Time-resolved ESI-CID-MS of nanodisc ions produced from a 1:1 mixture of GM2 and GM3 nanodiscs (10  $\mu$ M ganglioside) in a 200 mM aqueous ammonium acetate solution (pH 4.8, 22 °C) with hNeu3. (d) Plots of SA:IS abundance ratio measured for GM3 picodiscs (solid

red square) and GM2 picodiscs (solid blue diamond), GM3 nanodiscs (hollow red square), GM2 nanodiscs (hollow blue diamond).

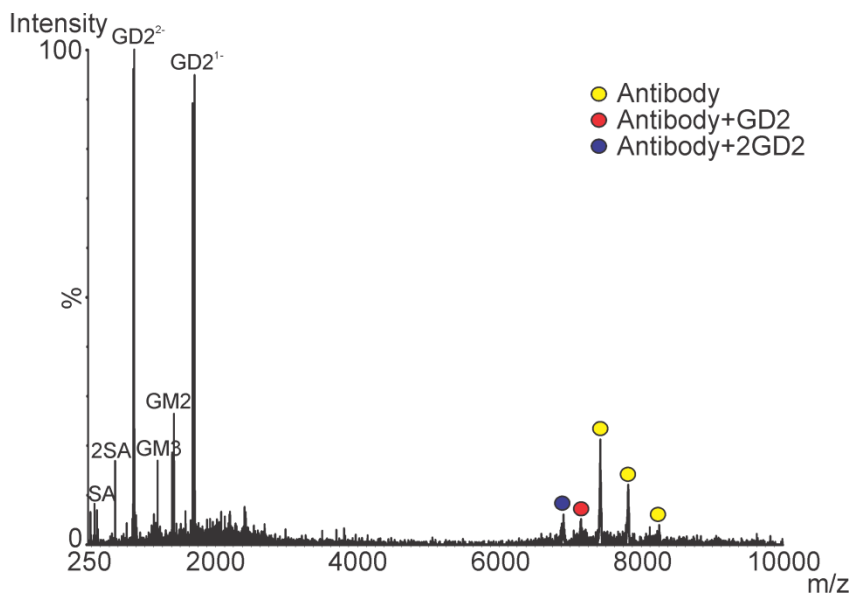


**Fig. S8.** CID mass spectrum of the  $(\text{mAb} + 2\text{GD2})^{22-}$  ion produced by ESI performed on aqueous ammonium acetate solution (200 mM, pH 6.8) of anti-GD2 mAb (1.5  $\mu\text{M}$ ) and GD2-containing picodisc (50  $\mu\text{M}$ ). CID was carried out in the Trap region using a collision energy of 100 V. The singly deprotonated ions of SA, 2SA, GM2 and GM3 are the result of secondary fragmentation of the  $\text{GD2}^{1-}$  and  $\text{GD2}^{2-}$  ions released from the  $(\text{mAb} + 2\text{GD2})$  complex.

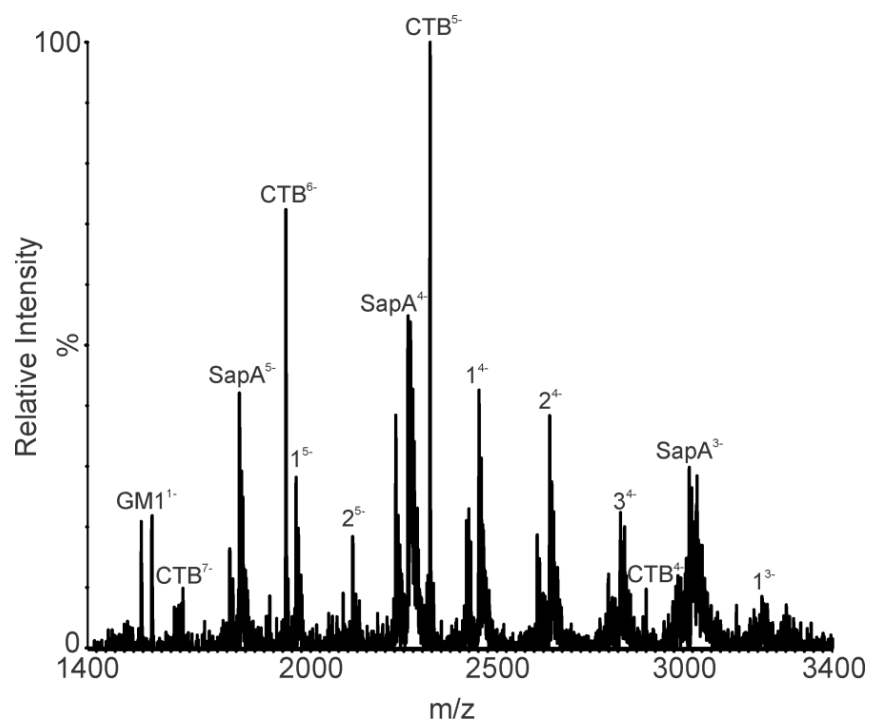


**Fig. S9.** CID mass spectrum of the  $(CTB_5 + 5GM1)^{16-}$  ion produced from aqueous ammonium acetate solution (200 mM, pH 6.8) of  $CTB_5$  (20  $\mu$ M) and GM1-containing picodisc (44  $\mu$ M). CID was carried out in the Trap region using a collision energy of 100 V. Peaks labelled 1, 2 and 3 correspond to SapA-POPC complexes with 1, 2 and 3 POPC molecules bound, respectively.

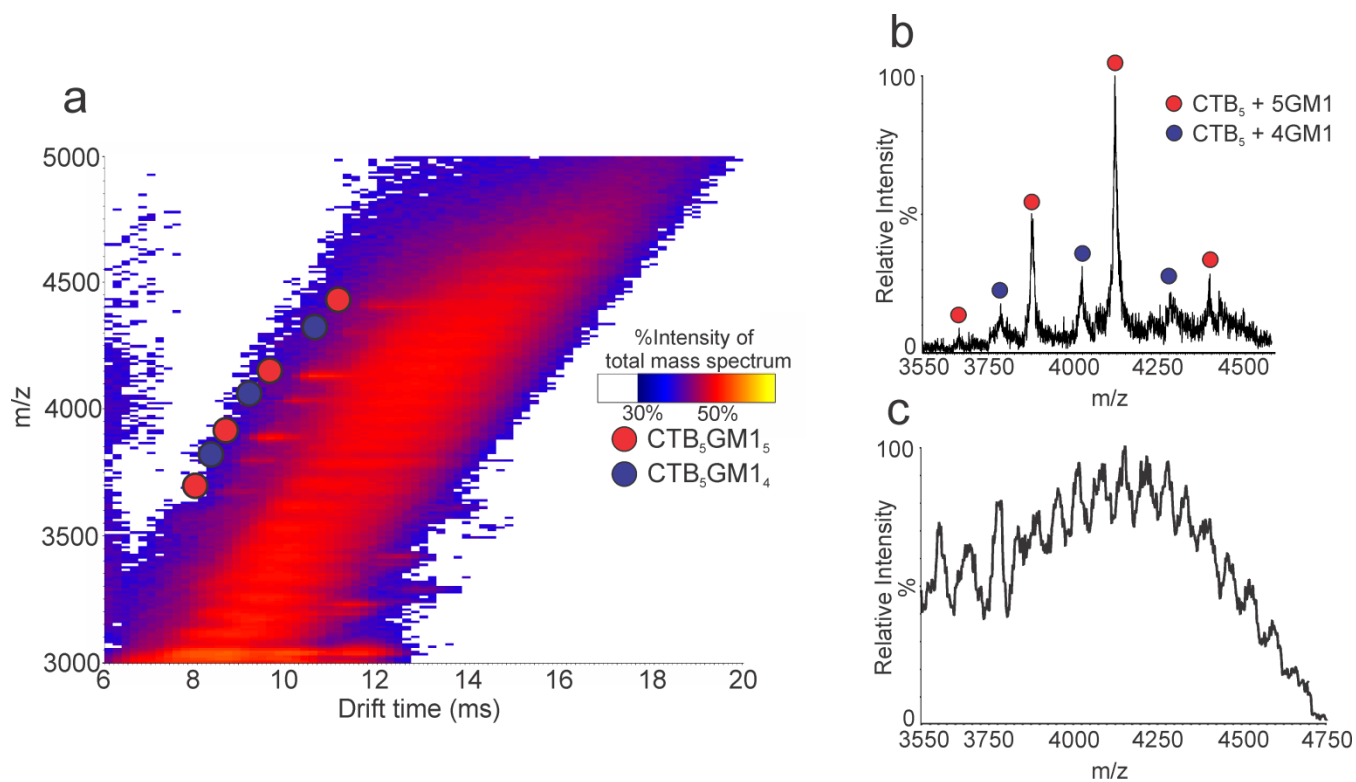


**Fig. S10.** (a) Intensity map of  $m/z$  versus IMS drift times measured for ions produced by ESI performed on aqueous ammonium acetate solution (200 mM, pH 6.8) of CTB<sub>5</sub> (20  $\mu$ M) and GM1 picodisc (44  $\mu$ M). Mass spectra of the ions corresponding to (b) (CTB<sub>5</sub> + 5GM1) and (CTB<sub>5</sub> + 4GM1) complexes and (c) the picodiscs extracted using Driftscope (v.2.5).

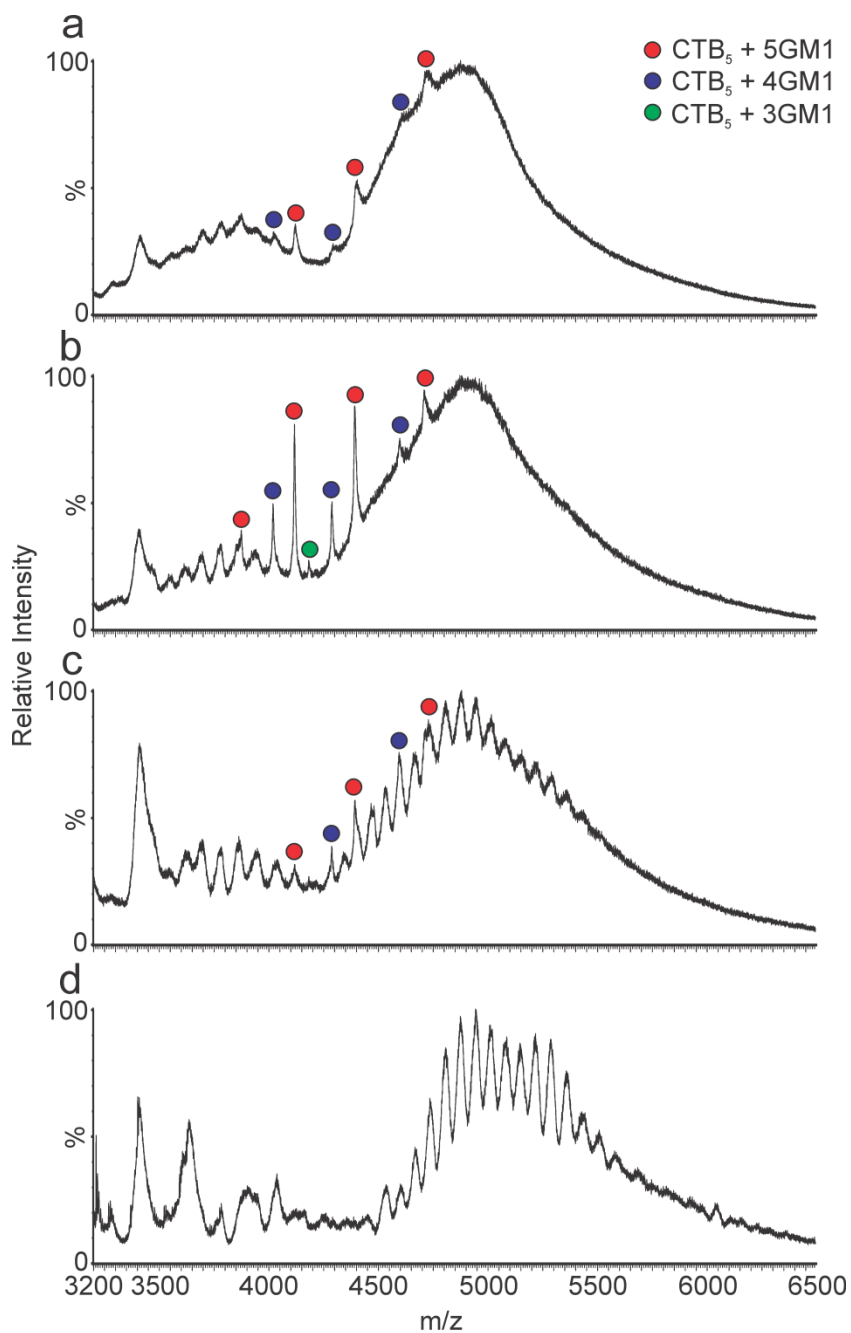


**Fig. S11.** ESI mass spectra acquired in negative ion mode for an aqueous ammonium acetate (200 mM, pH 6.8) solution of CTB<sub>5</sub> (20  $\mu$ M) and GM1 picodisc (44  $\mu$ M) at cone voltages of (a) 50 V, (b) 80 V, (c) 100 V and (d) 150 V.